

Esterolytic Antibodies as Mechanistic and Structural Models of Hydrolases—A Quantitative Analysis

Ariel B. Lindner¹, Se Ho Kim¹, Dan G. Schindler¹, Zelig Eshhar¹ and Dan S. Tawfik^{2*}

¹Department of Immunology
Weizmann Institute of Science
Rehovot 76100, Israel

²Department of Biological
Chemistry, Weizmann Institute
of Science, Rehovot 76100
Israel

Understanding enzymes quantitatively and mimicking their remarkable catalytic efficiency is a paramount challenge. Here, we applied esterolytic antibodies (the D-Abs) to dissect and quantify individual elements of enzymatic catalysis such as transition state (TS) stabilization, nucleophilic reactivity and conformational changes. Kinetic and mutagenic analysis of the D-Abs were combined with existing structural evidence to show that catalysis by the D-Abs is driven primarily by stabilization of the tetrahedral oxyanionic intermediate of ester hydrolysis formed by the nucleophilic attack of an exogenous (solution) hydroxide anion. The side-chain of TyrH100d is shown to be the main H-bond donor of the D-Abs oxyanion hole. The pH-rate and pH-binding profiles indicate that the strength of this H-bond increases dramatically as the neutral substrate develops into the oxyanionic TS, resulting in TS stabilization of 5–7 kcal/mol, which is comparable to oxyanionic TS stabilization in serine hydrolases. We show that the rate of the exogenous (intermolecular) nucleophilic attack can be enhanced by 2000-fold by replacing the hydroxide nucleophile with peroxide, an α -nucleophile that is much more reactive than hydroxide. In the presence of peroxide, the rate saturates ($k_{\text{cat}}^{\text{max}}$) at 6 s^{-1} . This rate-ceiling appears to be dictated by the rate of the induced-fit conformational rearrangement leading to the active antibody–TS complex. The selective usage of negatively charged exogenous nucleophiles by the D-Abs led to the identification of a positively charged channel. Imprinted by the negatively-charged TS-analogue against which these antibodies were elicited, this channel presumably directs the nucleophile to the antibody-bound substrate. Our findings are discussed in comparison with serine esterases and, in particular, with cocaine esterase (cocE), which possesses a tyrosine based oxyanion hole.

© 2002 Elsevier Science Ltd. All rights reserved

Keywords: catalytic antibodies; α -nucleophile; conformational changes; oxyanion hole; chemical rescue

*Corresponding author

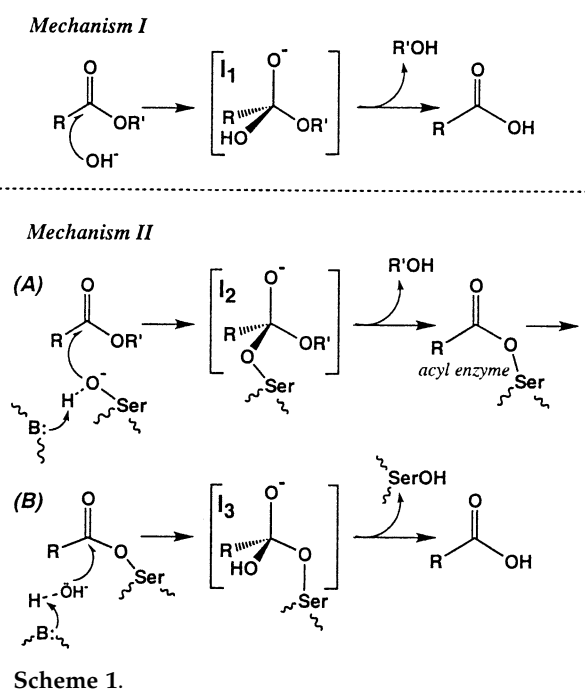
Present addresses: S. H. Kim, Antibody Engineering Lab., Central Research Center, Korea Green Cross Corp., 227, Gugal-Ri, Giheung-Eup, Yongin City, Gyunggi-Do 449-900, Korea; D. G. Schindler, Genzyme Transgenics Corp., 5, The Mountain Road, Framingham, MA 01701, USA.

Abbreviations used: TS, transition state; D-Abs, D2.3 and D2.4 antibodies; AChE, acetylcholinesterase; PBS, phosphate-buffered saline; TBS, Tris-buffered saline; BSA, bovine serum albumin; Nu, nucleophile; H-bond, hydrogen bond.

E-mail address of the corresponding author:
tawfik@weizmann.ac.il

Introduction

The remarkable catalytic efficiency of enzymes is the outcome of many forces and factors acting in concert. Separating these factors and quantifying the contribution of each to the overall rate acceleration of an enzyme is not a simple matter.¹ Enzyme models and catalytic antibodies in particular provide a unique opportunity to examine and quantify enzymatic forces and mechanisms of action individually. The first and foremost studied antibody-catalyzed reaction is ester hydrolysis, a reaction that proceeds *via* relatively low activation barriers and a well-defined singular tetrahedral, oxyanionic intermediate (**I**₁ in Mechanism I, Scheme 1).^{2,3} Antibodies raised against stable



analogues of this intermediate are routinely found to catalyze the hydrolysis of the corresponding esters (Figure 1).⁴ The vast majority of these esterolytic antibodies achieve catalysis by oxyanionic TS stabilization, i.e. by stabilizing the oxyanion I_1 intermediate and the TSs leading to and from it. Here, antibody-catalyzed hydrolysis proceeds *via* the same mechanism that prevails in spontaneous ester hydrolysis, an intermolecular nucleophilic attack of an exogenous hydroxide anion from solution (Mechanism I), with the difference being the stabilization of intermediate I_1 and the flanking TSs at the antibody's active-site.^{3,5}

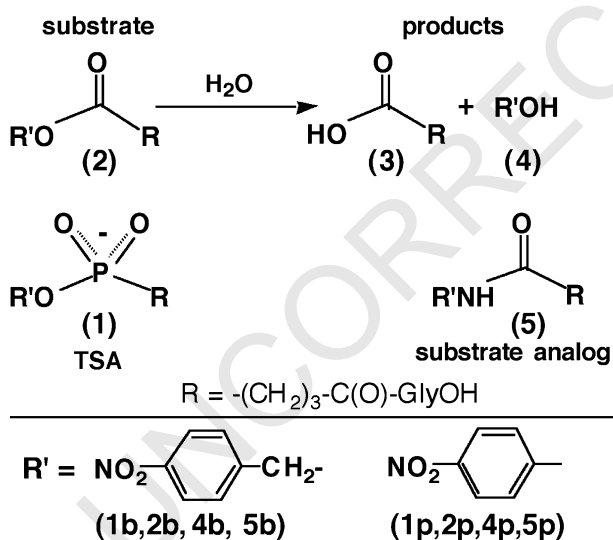


Figure 1. Structure of the compounds used in this study. The D-Abs were elicited against TSA **1b**. They catalyze the hydrolysis of esters **2** to give carboxylic acid **3** and the respective phenol or alcohol (**4**). Amides **5** were applied as non-hydrolysable substrate analogues.

In contrast, natural enzymes apply a more complex mechanism, combining a variety of catalytic forces, including preferential substrate alignment,⁶ endogenous nucleophiles (i.e. an intramolecular nucleophilic attack) and general-base catalysis (e.g. for deprotonation and activation of the deacylating water molecule), that complement oxyanionic TS stabilization. Unlike catalytic antibodies, in serine (or cysteine) hydrolases the nucleophilic attack is carried out by the alkoxide (or thiol) moiety of an active-site side-chain as an integral part (endogenous) of the active site (step A, Mechanism II). This is followed by a deacylation step mediated by an hydroxide anion generated *in situ* by the base-catalyzed proton elimination of an active-site water molecule (step B, Mechanism II).⁷ Mechanism II (Scheme 1), the central theme of which is the covalent acyl-enzyme intermediate, involves oxyanionic TSs and intermediates (I_2 and I_3) analogous to Mechanism I. The overall rate accelerations exhibited by esterolytic enzymes are generally in the range of 10^6 – 10^9 , although some esterases, such as acetylcholinesterase (AChE), can exhibit rate accelerations that are as high as 10^{13} .⁶ Natural esterases are therefore much more potent catalysts than catalytic antibodies that exhibit rate accelerations in the range of 10^3 – 10^5 . At the same time, the antibodies D2.3 and D2.4 (D-Abs) and most of the other known esterolytic antibodies apply a single catalytic force that is TS stabilization. In contrast, esterolytic enzymes apply a variety of catalytic forces that complement TS stabilization.

The above comparison of esterolytic enzymes *versus* antibodies raises several basic questions that are addressed here. (i) How do natural esterases and esterolytic antibodies compare in their efficiency of applying oxyanion stabilization to ester hydrolysis? (ii) Can the rate of the antibodies' intermolecular (exogenous) nucleophilic attack be enhanced significantly; and, can it rival the rate of the natural esterases? (iii) Is the rate of antibody catalysis affected by factors other than the chemistry (i.e. the nucleophilic attack), for example, by physical events such as conformational changes (as may be the case with many enzymes including esterases^{8–13})?

This study makes use of the D-Abs. Raised against *p*-nitrobenzyl phosphonate TSA **1b**,¹⁴ they catalyze the hydrolysis of the corresponding *p*-nitrobenzyl- and *p*-nitrophenyl-esters (**2b** and **2p**, respectively; Figure 1) with rate accelerations of 10^4 – 10^5 (Table 4) and are amongst the most potent esterolytic antibodies described to date.¹⁵

The crystal structures of the D-Abs in complex with TSA **2b** were solved, implicating two residues, Tyr100dH and Asn34L, as potential hydrogen-bond donors promoting the oxyanionic TS stabilization.¹⁶ The structures did not reveal any active-site residues that could potentially serve as endogenous nucleophiles^{16,17} but direct kinetic evidence supporting Mechanism I has not been obtained to date. In this study, we analyzed the

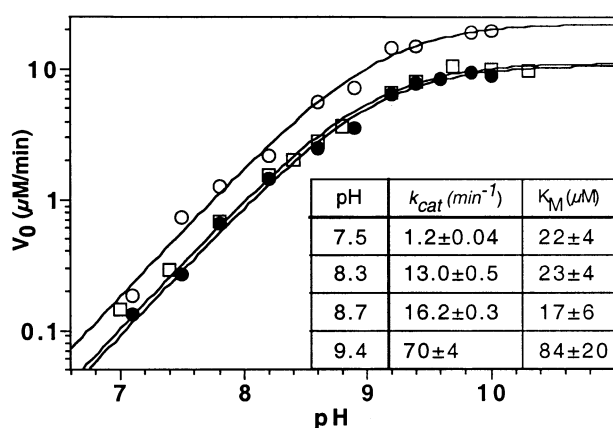


Figure 2. pH profile of the catalytic activity of the D-Abs. Rate of hydrolysis of ester **2p** was measured at different pH values with antibody D2.3 (\square) and D2.4 (\bullet), or, with antibody D2.4 in presence of $0.1 \mu\text{M}$ peroxide (\circ). The $\text{p}K_a$ value was derived from the plotted fit to equation (2) (see Experimental). Inset: kinetic parameters for antibody D2.4 at different pH values. Consistent with the pH-binding profile (Figure 3), at $\text{pH} \geq 10.5$, a decrease of the net antibody-catalyzed rates was observed though its quantification was impractical due to high background hydrolysis rates. Similarly, a full pH scale analysis of k_{cat} and K_M was unattainable at $\text{pH} > 9.5$ due to high background at high **2p** concentrations.

binding and kinetic pH profiles of the D-Abs and followed their activity in the presence of a set of α -nucleophiles that are far stronger than hydroxide.¹⁸ Our results support catalysis of D-Abs following Mechanism I and are not consistent with Mechanism II. Kinetic studies, supported by site-directed mutagenesis, ascertain the contribution of Tyr100dH to TS stabilization and quantify it. In contrast, Asn34L does not appear to play a significant role in TS stabilization nor in substrate

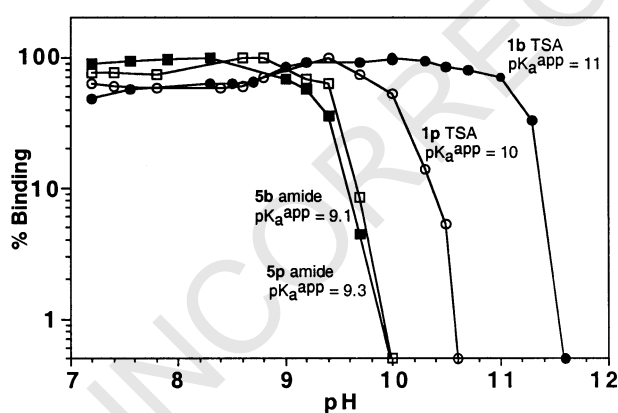


Figure 3. pH profile of antibody D2.4 binding activity. Binding of D2.4 to TSA **1b** (\bullet) and **1p** (\circ) and substrate analogues **5b** (\square) and **5p** (\blacksquare) was determined at various pH values by ELISA titration using the BSA-conjugates of these compounds. Apparent $\text{p}K_a$ values were deduced from the pH giving 50% of the maximal binding titer observed at $\text{pH} \leq 9$.

binding. Using peroxide, we have increased the efficiency of the exogenous nucleophilic attack (and hence k_{cat}) at neutral pH up to 2000-fold to a rate (6 s^{-1}) that approaches the catalytic efficiency of known natural esterases.^{19–21}

Results

The catalytic mechanism of catalysis of the D-Abs

The design of TSA **1b**, the immunizing hapten used to elicit the D-Abs, suggests that their mechanism should follow Mechanism I, whereby the negatively charged tetrahedral intermediate formed by the attack of a solution hydroxide anion (I_t in Mechanism I, Scheme 1) is stabilized by the antibodies' active-sites.⁵ Nevertheless, several antibodies raised against TSAs similar to **1b** were shown to follow Mechanism II.^{22,23} We therefore sought kinetic and other evidence that would confirm the mechanism of the D-Abs.

pH-rate profiles

The rate of the antibody-catalyzed ester hydrolysis in the pH range of 7–10.5 exhibits a linear phase (with a slope of 1) followed by an acid limb, reaching a plateau with an apparent kinetic $\text{p}K_a$ ⁷ of 9.0 (Figure 2). Mechanism I is consistent with the observed profile, whereby the antibody-catalyzed reaction is dependent on: (i) the concentration of hydroxide anions ($[\text{OH}^-]$). Specifically, as the studied pH range is much lower than the $\text{p}K_a$ of hydroxide, $\log[\text{OH}^-]$ is directly proportional to pH and hence results in a linear phase. (ii) An antibody active-site residue with an apparent $\text{p}K_a$ of 9.0, which, in its protonated state ($[\text{AbH}]$), is essential for substrate binding and catalysis, thus giving rise to the acid limb at $\text{pH} > 9$. Indeed, the data in Figure 2 fit a rate equation of the form: $\text{Rate} \propto [\text{OH}^-][\text{AbH}]$ (see Materials and Methods, equation (2)).

It should be noted that pH profiles similar to those shown in Figure 2 have been observed with other esterolytic antibodies. These were interpreted to implicate tyrosyl residues as the endogenous nucleophile in Mechanism II, although little additional evidence was provided.^{24–26} In the case of the D-Abs, analysis of the kinetic parameters at different pH values generally supports Mechanism I (Figure 2, inset). As the pH increases so does k_{cat} . This is in accordance with an increased hydroxide nucleophile concentration leading to a higher rate of formation of intermediate I_t and a higher rate of hydrolysis.²⁷ Unfortunately, this analysis is of restricted scope, as the very fast spontaneous rate of hydrolysis of ester **2p** prevented the determination of the discrete kinetic parameters (k_{cat} and K_M) at pH values above 9.5. Nevertheless, the pH-binding profiles of substrate analogues performed over a wide pH range (7–11.5; see below) indicate

Table 1. The complexes of D2.3 with various ligands: affinity constants *versus* pK_a

Ligand	K_a (M^{-1}) ^a	pK_a
1b	5×10^8	11.0
1p	5×10^7	10.0
5b	10^5	9.1
5p	1.25×10^4	9.3

^a Association constants were taken from Lindner *et al.*³⁰ and pK_a values from Figure 3 (this work).

that substrate binding (K_S) is indeed diminished above pH 9.0. Together, our data suggest that deprotonation of an antibody residue reduces substrate binding.

pH bonding profiles

Previously, we demonstrated the similarity between K_M and K_S as measured with the D-Abs in competitive hydrolysis assays between the **2p** and **2b** substrates (see Figure 4 of Tawfik *et al.*¹⁵). Direct binding measurements with non-hydrolyzable substrate analogues **5b** and **5p** show that substrate binding is dependent on a protonated antibody residue with a pK_a of about 9.0 (Figure 3). Notably, binding of TSAs **1p** and **1b** follows a similar regime yet exhibits higher apparent pK_a values. The order of pK_a values correlates quite well with the relative affinities by which these compounds bind the D-Abs (Table 1). The binding-pH profiles suggest that, due to a decrease in substrate binding, D-Abs catalysis would diminish at high pH values (Figure 3, **5b** and **5p** profiles). This is indeed reflected in the increase of K_M values

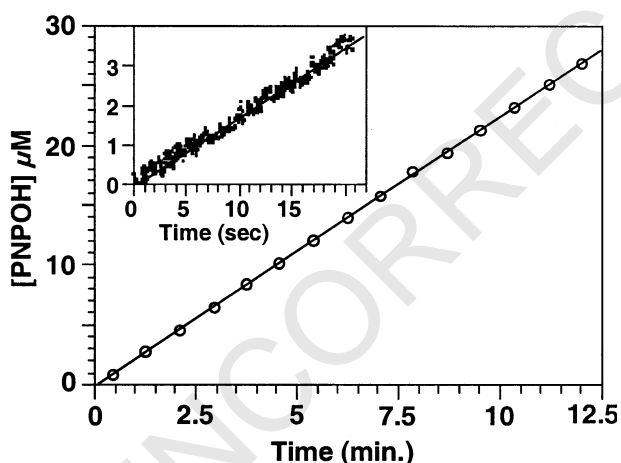


Figure 4. Rate of product release by antibody D2.4. Hydrolysis of ester **2p** (0.25 mM) in the presence of 0.2 μ M antibody D2.4 was measured in TBS (pH 8.3) by monitoring the release of the *p*-nitrophenol product (**4p**) using a microtiter plate reader (at 0.3–15 minutes). Inset: hydrolysis of ester **2p** (0.05 mM) in the presence of 1 μ M antibody D2.4 was measured in PBS (pH 7.05) using a stopped-flow apparatus (at 0–20 seconds).

at high pH (Figure 2, inset). Furthermore, at $pH \geq 10.5$, a decrease from the plateau of initial velocities (Figure 2) was observed, although the very fast rate of spontaneous hydrolysis of ester **2p** prevented its quantification.

The differences between the TSA (**1b** or **1p**) and the substrate analogues (**5b** or **5p**) are the configuration of the reaction core (the substrate's carbonyl group is planar as opposed to the tetrahedral phosphonate TSA) and the presence of the phosphonate's negatively charged oxyanion.²⁸ The nucleophilic attack on the ester substrate to give intermediate I_1 leads to a similar change. We suggest that in both cases, the added negative charge leads to a stronger H-bond that is apparent in the increased apparent pK_a of the active-site residues acting as donors in this interaction.

Effect of peroxide on reaction rates

The effect of peroxide anion, an α -nucleophile that has a charge similar to that of hydroxide, yet is far more reactive, is in agreement with Mechanism I. First, as is observed with hydroxide, the increase in rate of the antibody-catalyzed reaction largely mirrors the increase observed with peroxide in solution in the absence of antibody (Figure 5(a) and (b)). Second, the pH-rate profile in the presence of peroxide parallels that observed with hydroxide (Figure 2). This supports the conclusion that the peroxide anion (O_2H^-) rather than its neutral form serves as the active nucleophile. As is the case with hydroxide, the concentration of the anionic nucleophilic form ($\log [O_2H^-]$) increases linearly at the pH range studied, which is well under the pK_a of peroxide (11.6). This gives rise to the linear phase of the pH-rate profile (Figure 2). Moreover, the same apparent pK_a is observed with both hydroxide and peroxide, supporting our conclusion that the pH profiles reflect the deprotonation of an active-site residue and are not dependent on the nature of the nucleophile. The possibility that product-release becomes rate-limiting at high pH values and is thus responsible for the rate-plateau observed at $pH > 10$ (Figure 2), is ruled out, as the plateau rates in presence of peroxide are consistently higher than those observed for the hydroxide-mediated hydrolysis. The rate increase of the antibody-catalyzed hydrolysis in the presence of a stronger nucleophile (peroxide) indicates that the nucleophilic attack by the exogenous hydroxide, leading to the I_1 intermediate, is rate-limiting. Arguably, this rate-limiting step could correspond to the deacylation step of Mechanism II (Step B, Scheme 1), which could be catalyzed by exogenous hydroxide anions. In such a case, however, an initial burst of product release should be observed, corresponding to the fast accumulation of the acyl-enzyme intermediate.⁷ Such bursts are indeed observed in esterases and amidases that apply Mechanism II and, in particular, with *p*-nitrophenyl esters, for which acylation is very fast and deacylation is

Table 2. Contribution of oxyanion hole residues to D-Ab binding and catalysis

Fv antibody fragment	Catalysis (% of wild-type) ^a	TSA 1p binding (% of wild-type) ^b
Wild-type	100	100
AsnL34 → Gly	115 ± 5	65 ± 7
TyrH100d → Phe	<0.1	<0.1
TyrH100d → Gly	<0.1	<0.1
TyrH100d → Lys	<0.1	4 ± 1
TyrH100d → Ser	8 ± 2	4 ± 1

^a Activities for wild-type and the AsnL34 → Gly mutant were obtained from the k_{cat} values for ester **2p**. Catalytic activity of the TyrH100d was determined by catELISA as their activity was too low to be detected with the soluble substrate.

^b Binding of **1p** TSA was determined by ELISA using **1p** conjugated to BSA.

therefore rate-limiting. However, no burst of product release is observed with the D-Abs, on either a second or on a minute time-scale (Figure 4). Burst kinetics is absent both with peroxide and with hydroxide, even though the reaction rate with hydroxide is 60-fold slower. Thus, Mechanism II is further disproved by the fact that no burst is observed even when the rate of nucleophilic attack, and hence the rate of hydrolysis, is considerably reduced.

Site-directed mutagenesis of TyrH100d and AsnL34

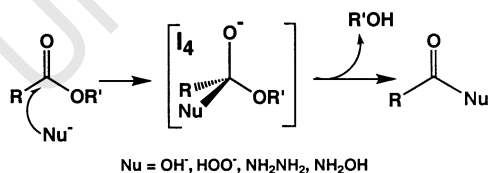
TyrH100d and AsnL34 were implicated by the D-Abs crystal structures as H-bond donors to the TS oxyanion (Figure 8).¹⁶ To assess the contribution of these residues to catalysis by the D-Ab, various mutants were generated in the framework of a recombinant Fv fragment consisting of D2.4 variable heavy chain and D2.3 variable light chain.²⁹ Mutation of asparagine L34 to glycine had almost no effect on binding or catalysis, suggesting that this residue does not contribute significantly to the oxyanion hole of the D-Abs. In contrast, the relatively conserved mutation of tyrosine H100d to phenylalanine reduced both binding and catalysis by more than 1000-fold (Table 2). Two other mutants of TyrH100d exhibited some residual binding and catalytic activity. Interestingly, these mutations introduced residues that can serve as H-bond donors (lysine and serine). These results confirm the assignment of an H-bond between TyrH100d and the ester substrate's carbonylic oxygen atom in the crystal structure of the antibody-substrate complex¹⁶ and suggest that TyrH100d is the main contributor to the catalytic mechanism of the D-Abs. The identification of TyrH100d is also consistent with the pH profiling results. Although the pK_a of the hydroxyl group of tyrosine is nor-

mally around 10, the apparently reduced pK_a observed here (9.0) may be due to our inability to measure the pK_a of TyrH100d directly (our results are limited to a kinetic pK_a at a single substrate concentration (Figure 2) or refer to the antibody-substrate analogue complex (Figure 3)). It is possible that, as is often the case, in the active-site microenvironment, the pK_a of TyrH100d is reduced due to local medium or electrostatic effects.

The D-Abs exhibit selectivity towards exogenous nucleophiles

Tetrahedral, negatively charged intermediates can be formed by the attack on the ester's carbonyl group by various nucleophiles (**I₄** in Scheme 2). Given the similarity in configuration and charge to **I₁** (Scheme 1) and the TSA against which the D-Abs were elicited (Figure 1), these intermediates and the flanking TSs could be stabilized by the D-Abs, leading to the accelerated rate of ester **2p** cleavage (Scheme 2).

We examined small α -nucleophiles that, relative to their pK_a values, are considerably more reactive than hydroxide (Figure 5, Table 3).¹⁸ We found that, at the D-Ab active sites, the catalytic reaction proceeds in the presence of peroxide as efficiently as with hydroxide (Figure 5(a) and (b)). Peroxide is a much better nucleophile than hydroxide and, unlike hydroxide, its concentration can be increased without raising the pH. Consequently, the antibody-catalyzed rates (k_{cat}) are significantly faster than with hydroxide. However, as the effect of peroxide on the antibody-catalyzed and on the uncatalyzed background reaction is essentially the same, the rate accelerations ($k_{\text{cat}}/k_{\text{uncat}}$) of the D-Abs with hydroxide or peroxide are similar (15% higher and 55% lower for D2.4 and D2.3, respectively; Table 3). This is not the case with hydrazine, hydroxylamine or azide. These nucleophiles exhibit a much lower rate (if any) in the presence of the D-Abs, while in solution, they react with ester **2p** at considerable rates. So much so, that in the presence of D2.3 no cleavage of ester **2p** is observed (beyond the basal reaction observed in buffer) with hydrazine or hydroxylamine at concentrations up to 10⁴-fold higher than hydroxide (Figure 5(c) and (d); Table 3). The D-Abs exhibit no reduction in activity after prolonged incubation



Scheme 2.

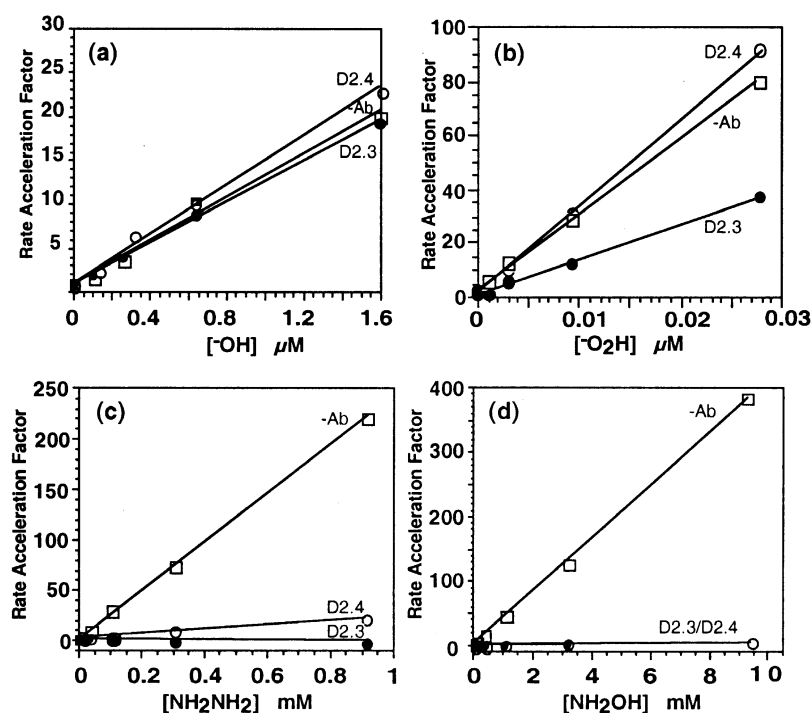


Figure 5. The effect of different exogenous nucleophiles on **2p** hydrolysis. Hydrolysis of ester **2p** was followed in buffer (with no antibody; □) or in the presence of antibody D2.3 (●) or D2.4 (○). Rate-acceleration factors are the ratios of net initial rates observed in the presence of the nucleophile at a given concentration and in its absence. Nucleophile concentrations are given for their active, deprotonated form (note the different concentration ranges of each nucleophile).

with these nucleophiles at the concentration range studied (0–100 mM) as judged by ELISA binding tests to substrate analogue **5p** and TSA **1b**. Thus, the lack of activity of the D-Abs with hydroxylamine, hydrazine or azide is not due to inactivation or inhibition of the antibodies. Rather, these nucleophiles fail to react with ester **2p** when placed at the D-Abs active sites. We ascribe the preference towards negatively charged nucleophiles (hydroxide and peroxide) to a positively charged tunnel we have identified that leads to the active site of the D-Abs. We propose that this channel directs the attacking nucleophile to the ester substrate (see Discussion and Figure 7).

Saturation of the peroxide-assisted D-Abs rates

The ability of the D-Abs to utilize peroxide provides a unique opportunity to examine how the rate of the antibody-catalyzed hydrolysis changes when the efficiency of the nucleophilic attack is enhanced by several orders of magnitude. Using a stopped-flow apparatus, the rate of product release

was measured at increasing concentrations of peroxide. Saturation kinetics was observed with a similar plateau level for both antibodies at $k_{\text{cat}}^{\text{max}}$ of 6 s^{-1} (Figure 6). This pattern led us to examine whether the observed kinetics obey the Michaelis–Menten model with respect to an antibody–peroxide complex. The data show systematic deviations from this model. Moreover, the apparent $K_{\text{M}}^{\text{O}_2\text{H}^-}$ obtained from these poor fits ($1 \mu\text{M}$ for D2.4 and $3.5 \mu\text{M}$ for D2.3; Figure 6) represents an unreasonably high affinity to the peroxide anion (compared to the substrate analogues (5; Table 1) or to the ester substrates: $K_{\text{M}}^{2\text{p}} = 33 \mu\text{M}$ for D2.3; $K_{\text{M}}^{2\text{p}} = 23 \mu\text{M}$ for D2.4). In theory, the observed peroxide-mediated rate ceiling could also reflect a two-step mechanism (Mechanism II), whereby a very fast acylation step is followed by a rate-limiting, hydroxide-mediated deacylation. At high concentrations of peroxide, when the rate of deacylation is greatly enhanced, the rate of acylation could become limiting, thus giving rise to the 6 s^{-1} rate ceiling. This scenario, however, would be expected to yield a single-turnover burst of

Table 3. The reactivity of exogenous nucleophiles

Nucleophile ^a	pK _a	Buffer ($\times 10^6 \text{ M}^{-1}$) ^b	Antibody D2.3 ($\times 10^6 \text{ M}^{-1}$) ^b	Antibody D2.4 ($\times 10^6 \text{ M}^{-1}$) ^b
OH ⁻	15.4	13	12	14
O ₂ H ⁻	11.6	2800	1270	3200
NH ₂ NH ₂	8.1	0.24	0	0.008
NH ₂ OH	6.0	0.45	0	0.006
N ₃ ⁻	4.0	1×10^{-3}	n.d.	0.01×10^{-3}

^a A linear correlation links the nucleophilicity of most nucleophiles to their pK_a values. However, the reactivity of the α -nucleophiles cited above (i.e. excluding OH⁻) is far higher than predicted from their pK_a values (e.g. 10^3 -fold for hydroxylamine).¹⁸

^b Results are given in molar reactivity, the rate acceleration factor at 1 M nucleophile as extrapolated from Figure 5. n.d., not determined.

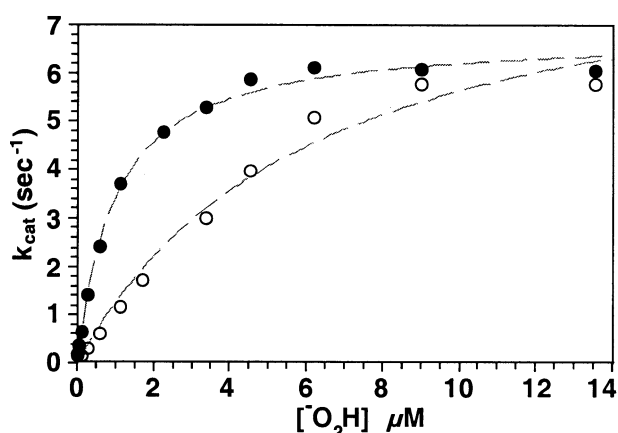


Figure 6. The effect of peroxide on catalysis by the D-Abs. Using a stopped-flow apparatus, the release of *p*-nitrophenolate product **4p** was measured at increasing peroxide concentrations in the presence of D2.3 (○) and D2.4 (●). The net antibody-catalyzed rates (v_0) were used to determine k_{cat} (see Experimental). The hatched-line represents an attempt to fit the data to the Michaelis-Menten model whereby:

$$k_{\text{cat}}^{\text{max}} = k_{\text{cat}}[\text{O}_2\text{H}^-]_0 / ([\text{O}_2\text{H}^-]_0 + K_M^{\text{O}_2\text{H}^-}).$$

product release when the rate of acylation is rate-limiting (i.e. with hydroxide as the nucleophile). However, such a burst is not observed with the D-Abs (Figure 4). An alternative explanation is based on our previous observation of rate-limiting conformational changes in the course of TSA binding to the D-Abs. The rate of these induced-fit isomerisations is essentially identical with the rate ceiling observed here with peroxide (6 s^{-1} ; Lindner *et al.*³⁰). The possibility that a conformational change dictates the rate-ceiling of the D-Abs is further discussed below.

Discussion

This study aims at deciphering the catalytic mechanism of the D-Abs and quantifying the contribution of various elements of the mechanism to their rate acceleration. A comparison is then made between the contributions of the same element to catalysis by natural esterases.

TS stabilization by the D-Abs

Mechanism I emerges as the simplest mechanism that is in agreement with the kinetic data, the results of site-directed mutagenesis and the structural analysis of the D-Abs. Our results also suggest that the oxyanion hole of the D-Abs is the major source for their catalytic power. The oxyanion hole is dependent on the protonated form of TyrH100d active-site residue with an apparent $\text{p}K_a = 9\text{--}11$ depending on the complexed ligand and the nature of the analysis (Figures 2 and 3). TyrH100d is positioned in a favorable orientation within H-bond distance (2.8 Å) from the TSA's phosphonate group (Figure 8), a theme shared with other esterolytic antibodies.⁵ The structure of the D-Abs in complex with substrate-analogue **5b** indicates that the same tyrosyl residue is critical for both TSA and substrate recognition,¹⁷ forming an H-bond with the substrate analogue scissile carbonyl oxygen atom (at a distance of 2.6 Å). In contrast, Asn34L, which was previously implicated with the oxyanion of the D-Abs,¹⁶ appears to play a minor role, if any, in substrate binding and TS stabilization (Table 2). This may be reflected in the structure of the substrate-antibody complex (1YEF in PDB) as 3.8 Å separate the asparagine's δ -amide proton donor and the scissile bond carbonyl oxygen atom (compared to 2.6 Å distance from the oxygen atom of TyrH100d). The pH-binding

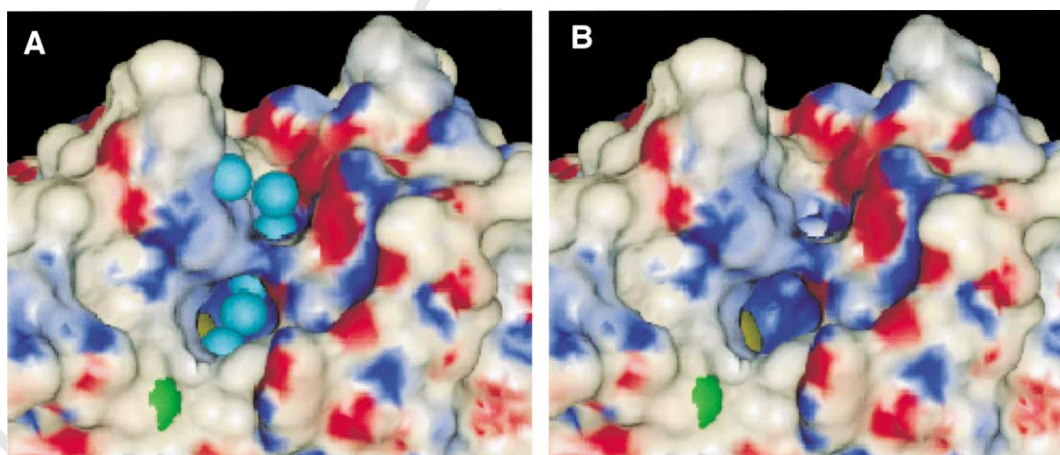


Figure 7. Surface charge of antibody D2.3 in complex with substrate analogue **5b**. The surface was calculated using the 2.00 Å resolution 1YEF PDB structure,¹⁷ treating the antibody and **5b** as a single body. Surface charge was calculated using Delphi⁵⁷ and Insight II software (Accelrys). The active-site view is taken from the direction of substrate entry.¹⁷ The outermost atom of **5p** is marked in green; the rest of it is either buried or comprises part of the surface. The assumed site of the nucleophilic attack (the ester's carbonyl group) lies at the very bottom of this channel and is marked in yellow. (a) The channel leading the nucleophile entry into the active site is threaded with structured water molecules (light blue spheres). (b) The channel shown in (a), excluding the water molecules.

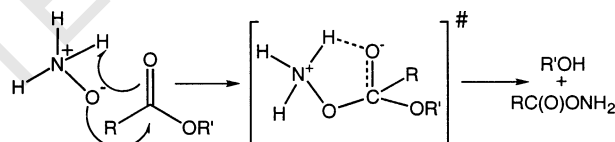
profiles reveal a 1.6–1.9 unit difference in pK_a between the substrate–antibody and the TSA–antibody complexes (Figure 3 and Table 1). Thus, the negative charge marking the difference between the substrate and the TSA (and hence the actual TSs of the reaction) strengthens the tyrosyl-oxyanion H-bond dramatically, thus rendering it the key residue in the D-Abs' oxyanion hole.

Nucleophile discrimination and channeling

As the rates of the D-Abs are normally limited by the hydroxide nucleophilic attack, the antibody-catalyzed rate could, in principle, be improved by applying more effective nucleophiles. Of a variety of α -nucleophiles that enhance the rate of ester hydrolysis in solution (Figure 5, Table 3),¹⁸ the D-Ab active sites make use of the oxyanionic peroxide only. Other nucleophiles, hydrazine, hydroxylamine and azide, are largely, or even completely, inactive (Figure 5). The nucleophile discrimination appears to be yet another manifestation of the ability to tailor the specificity of action of catalytic antibodies. Its origins seem to be in the way the D-Ab combining sites were selected to recognize the negatively charged TSA. When bound to the D-Ab active site, the TSA's phosphonate oxyanions are within H-bonding distances and angles from TyrH100d and AsnL34, (the proS oxygen atom, O1) (Figure 8(a)), or TrpH95 (the proR oxygen atom, O2). The structure of D2.3 with substrate-analogue **5b** indicates that the substrate's carbonyl oxygen atom overlaps the position of O1, while the O2 position remains unoccupied and is linked by a water-threaded channel leading to the antibody's surface, perpendicular to the substrate entry site. The structured water molecules were suggested to delineate the path of hydroxide nucleophile entry into the active site (Figure 7(a)).¹⁷ Our analysis suggests that the strong bias towards oxyanionic nucleophiles may result from the surface electrostatics of the active-site water-threaded channel. We find that, owing to the presence of the heavy-chain germline residues HisH35, ArgH50, and ArgH94, this channel is highly positively charged (Figure 7(b)). This is probably the result of these antibodies being elicited against the negatively charged TSA **1b**.³¹ Notably, the D-Abs were selected out of hundreds of other TSA-binding antibodies that had lower or no catalytic activity.¹⁴ The positively charged channel may be part of the selected catalytic machinery in steering and facilitating the entry of the negatively charged nucleophile into the active site. To establish this link, we analyzed the sequence of 20 catalytic antibodies raised against TSA **1b** in three different mouse strains (Balb/c, NOD and SJL) (our unpublished results). The abundance of HisH35 (80%) and ArgH94 (80%) are in agreement with their appearance in the known mouse heavy-chain variable (V_H) region,³² 50% and 80%, respectively. In contrast, the high abundance of ArgH50 (65%) in our sequenced antibodies (regardless of

their germline origin) is distinctive compared to its 10% abundance in all known mouse V_H sequences. The ArgH50 guanidinium moiety is exposed to the D-Abs active site, and is located 5.5 Å away from the substrate analogue scissile bond carbonyl group, within hydrogen bond distance (2.9 Å) from the water molecule closest to the same substrate carbonyl group (4.0 Å). Thus, ArgH50 may have been selected in direct response to the negatively charged hapten **1b** and by the direct screening for catalytic activity.¹⁴ Further, in order to reach the ester substrate and attack it, the nucleophile needs to displace the structured water molecules residing in the channel. Nucleophile discrimination could therefore stem from favorable electrostatic interactions between the anionic nucleophiles and the positive channel that compensate for the considerable energy loss involved in displacing these structured water molecules.

It should also be noted that the high reactivity of hydroxylamine towards esters such as *p*-nitrophenyl acetate is primarily due to its zwitterionic form. In this configuration, the nucleophile is the oxyanion and the protonated amine H-bonds to the TS's oxyanion (Scheme 3).³³ The tightly packed active site of the D-Abs may disfavor this spatially demanding configuration. Hydrazine may follow a similar mechanism, yet the equivalence of its two amine groups makes them indistinguishable. The azide nucleophile (N_3^-), due to its long and rigid rod-like shape, may not fit into the active site in the orientation required for the nucleophilic attack. In addition, although carrying an overall negative charge, its charge distribution (similar to that of hydroxylamine) includes a positive charge that might hinder its entrance through the narrow, positively charged channel.



Scheme 3.

Finally, the observed nucleophile discrimination calls for caution in the mechanistic interpretation of the effect of exogenous nucleophiles. Similar complexities were described for an enzyme model.³⁴ Specifically, as shown here, the lack of rate acceleration with a particular nucleophile^{26,35} may not necessarily indicate that an exogenous hydroxide nucleophile does not take part in the rate-limiting step.

The rate-ceiling of the D-Abs

We have addressed the question of whether the contribution of the exogenous (intermolecular) nucleophilic attack is additive to the contribution of the oxyanion stabilization by supplementing the D-Abs with highly reactive α -nucleophiles.

Table 4. Kinetic constants of ester hydrolysis by D2.3, D2.4 and cocE

Catalyst, substrate	D2.4 ^a , ester 2p	D2.3 ^a , ester 2b	cocE, cocaine
k_{uncat} (s ⁻¹)	8×10^{-6}	5×10^{-7}	1.2×10^{-6} ^b
k_{cat} (s ⁻¹)	0.22	0.05	7.8 ^c
$k_{\text{cat}}/k_{\text{uncat}}$	2.7×10^4	1.1×10^5	6.5×10^6

^a Tawfik *et al.*¹⁵
^b Landry *et al.*⁵⁸
^c Larsen *et al.*²¹

Our approach is analogous to the study of natural enzymes in which an endogenous catalytic residue is removed by site-directed mutagenesis. The catalytic activity of the mutants can often be restored with a soluble catalytic group that resembles the truncated active-site residue to rates only 100–300-fold lower than that of the intact enzyme.^{36–38} The selectivity of the D-Abs towards oxyanionic nucleophiles and the high nucleophilicity of peroxide enabled this approach. The rates of the D-Abs increase with the addition of peroxide but reach saturation at $k_{\text{cat}}^{\text{max}} = 6(\pm 1) \text{ s}^{-1}$ (compared with $k_{\text{cat}}^{\text{(D2.3)}} = 0.003 \text{ s}^{-1}$ and $k_{\text{cat}}^{\text{(D2.4)}} = 0.012 \text{ s}^{-1}$ in the absence of peroxide at the same neutral pH; Figure 6). Previously, we measured the rates of conformational isomerisations of the D-Abs induced by binding of TSA **1b** or **1p** by stopped-flow fluorescence quenching. These experiments indicated an induced-fit mechanism whereby an initial low-affinity encounter complex isomerises to give a 60-fold higher affinity complex. This isomerisation is governed by an apparent rate of 6 s^{-1} (Lindner *et al.*³⁰), a rate constant that is essentially identical with the rate observed in the peroxide-catalyzed hydrolysis at saturation. Thus, unless this identity of rates is haphazard, the observed $k_{\text{cat}}^{\text{max}}$ of 6 s^{-1} (Figure 6) may suggest that a similar isomerisation follows substrate binding and the formation of TSA-like intermediate **I**₁ (Mechanism I). This places a 6 s^{-1} kinetic barrier on the catalytic cycle of the D-Abs. This barrier is not met under ordinary conditions, i.e. with hydroxide as the exogenous nucleophile, where the nucleophilic attack is clearly rate-limiting (see above). With peroxide, however, the rate of nucleophilic attack is increased (500 and 2000-fold, with

D2.4 and D2.3, respectively, at neutral pH) and the conformational isomerisation does become rate-limiting. This finding delineates the catalytic role of the conformational isomerisation of the D-Abs and confirms the notion that antibody–TSA interactions truly reflect the antibodies' interaction with the actual TS.³⁰

Comparison of the D-Abs to esterolytic enzymes

Oxyanion hole and TS stabilization

The specific free energies for the complexation of the D-Abs with the TSA ($\Delta G_{\text{TSA}}^0 - \Delta G_{\text{S}}^0$) are almost identical with the reduction in the activation energy barrier derived for the D-Abs from their rate acceleration ($\Delta G_{\text{cat}}^{\ddagger} - \Delta G_{\text{uncat}}^{\ddagger}$) (Table 4). This tight correlation suggests that the active sites of the D-Abs convert binding energy into catalysis with ~100% efficiency. How do these values compare with the efficiency of oxyanion stabilization in natural hydrolases? Oxyanion stabilization mediated, as in the D-Abs, by a tyrosine residue has been demonstrated recently in the serine-hydrolase cocaine esterase 1 that applies Mechanism II (cocE; Table 5; Figure 8(b)),²¹ as well as in a number of prolyl oligopeptidases.^{39–41} The tyrosyl contribution to the mechanism of these peptidases was assessed by a Tyr-to-Phe mutation exhibiting up to ~1000-fold (4.2 kcal/mol : 1 cal = 4.184 J) decrease in k_{cat} .^{40,41} A similar (or possibly higher) decrease in activity is observed with the D-Abs upon mutation of tyrosine H100d to phenylalanine (Table 2). Thus the contribution of TS stabilization to the D-Ab catalysis (5.3–7.0 kcal/mol; Table 5)

Table 5. Binding energies of the D-Abs and their contribution to catalysis

Ab	1b TSA and 2b ester (kcal/mol)		1p TSA and 2p ester (kcal/mol)	
	$\Delta G_{\text{TSA}}^0 - \Delta G_{\text{S}}^0$ ^a	$\Delta G_{\text{cat}}^{\ddagger} - \Delta G_{\text{uncat}}^{\ddagger}$ ^b	$\Delta G_{\text{TSA}}^0 - \Delta G_{\text{S}}^0$ ^a	$\Delta G_{\text{cat}}^{\ddagger} - \Delta G_{\text{uncat}}^{\ddagger}$ ^b
D2.3	7.0	7.0	4.5	5.3 ^c
D2.4	6.3	6.3	4.8	6.1 ^c

^a Derived from binding association constants for the TSA *versus* the substrate (K_{TSA} and K_{S} , respectively¹⁵) using $\Delta G_{\text{TSA}}^0 - \Delta G_{\text{S}}^0 = -RT(\ln K_{\text{TSA}}/K_{\text{S}})$.

^b Derived from the rate constants at pH 8.3 for the antibody-catalyzed hydrolysis (k_{cat}) *versus* the rate constant of the uncatalyzed rate of hydrolysis extrapolated to zero-buffer concentration (k_{uncat})¹⁵ using $\Delta G_{\text{cat}}^{\ddagger} - \Delta G_{\text{uncat}}^{\ddagger} = -RT(\ln k_{\text{cat}}/k_{\text{uncat}})$.

^c In the case of the *p*-nitrophenyl pair (TSA **1p** and ester substrate **2p**), the reduction in activation energy ($\Delta G_{\text{cat}}^{\ddagger} - \Delta G_{\text{uncat}}^{\ddagger}$) exceeds the expected contribution from the relative affinities to the D-Abs ($\Delta G_{\text{TSA}}^0 - \Delta G_{\text{S}}^0$). This suggests that **1p** (unlike the immunizing hapten **1b**; Figure 1) is not the optimal TS mimic for the antibody-mediated **2p** ester hydrolysis as discussed by Tawfik *et al.*¹⁵

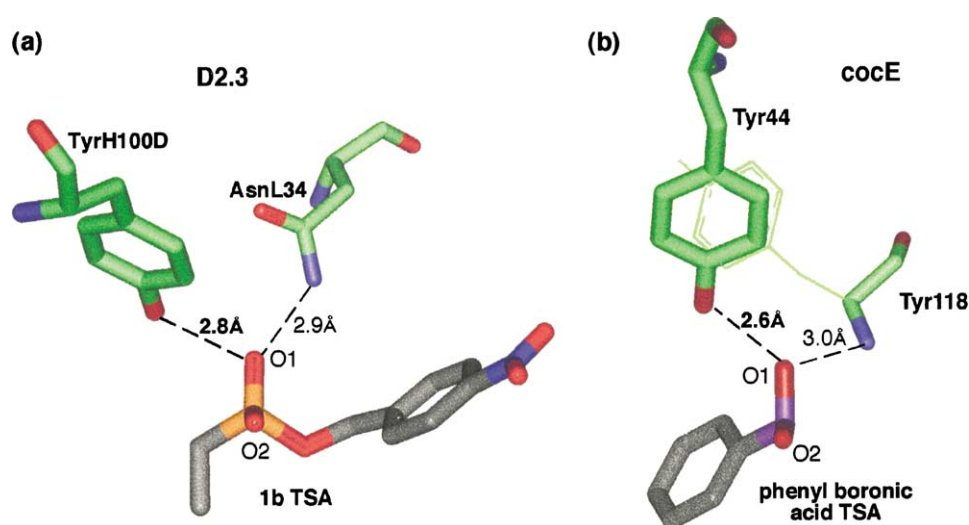


Figure 8. The oxyanion holes of antibody D2.3 and cocE. (a) The D2.3 residues implicated in TS stabilization are deduced from the structure of D2.3 in complex with TSA **1b** (1YEC in PDB¹⁶); O1 represents the TS oxyanion and O2 represents the putative position of the nucleophile. (b) The oxyanion hole residues of cocE as suggested by its crystal structure with phenyl boronic acid (1JU3 in PDB²¹). The side-chain of Tyr44 and the backbone of Tyr118 are depicted with their hydrogen bonds to the putative TS. O1 represents the TS oxyanion whereas O2 represents the hydroxyl nucleophile of Ser117 (the Tyr118 side-chain, represented in wireframe, is not involved in TS stabilization).

compares favorably with the enzymatic homologous oxyanion hole. The estimated value for oxyanion hole contribution in other serine hydrolases (e.g. AChE, 5–7 kcal/mol;⁶ and subtilisin, 5 kcal/mol)¹ is remarkably similar to the values measured for the D-Abs even though their oxyanion hole architecture is very different. The H-bond donors of AChE are backbone amide groups and those of subtilisin are both a main-chain amide group and an asparagine side-chain). Furthermore, the contribution of a single side-chain to oxyanion stabilization of hydrolases is distinctly lower than the contribution of Tyr100d in the D-Abs, as revealed by mutagenesis; for example: subtilisin N155A, 2–3 kcal/mol;^{42,43} papain N19A, ~3 kcal/mol;⁴⁴ cutinase Ser42A, ~3 kcal/mol;⁴⁵ oligopeptidase B Y452E, 3–4 kcal/mol;^{40,41,46} and *Escherichia coli* signal peptidase Ser88A, ~4 kcal/mol.⁴⁷ It appears therefore that the D-Abs achieve enzyme-like efficiency in applying one fundamental enzymatic feature, that of the oxyanion hole. They do so with a chemistry and structure similar to that of enzymes,^{21,39–41} indicating the convergent evolution of oxyanion holes in two completely different biological systems: on one hand, antibodies that evolved in a mammalian system to bind a phosphonate TSA, and on the other hand, a bacterial enzyme that evolved to hydrolyze cocaine.⁴⁸

Contribution of the nucleophilic attack

The esterase cocE exhibits a rate enhancement of 6.5×10^6 .²¹ This is within the range of most natural esterases that exhibit rate accelerations ($k_{\text{cat}}/k_{\text{uncat}}$) of 10^6 – 10^9 fold. The D-Abs, however, exhibit ca 100-fold lower accelerations than cocE (Table 4). The uncatalyzed hydrolysis rates of both the

benzyl ester substrates of the D-Abs and cocE are comparable (Table 4) and so are their oxyanion holes (Figure 8). Hence, cocE may serve as an adequate reference to the D-Abs. Given the above similarities, we propose that the energy gained by TS stabilization by the D-Abs (Table 5) is comparable to the contribution of oxyanionic stabilization to the rate enhancement of cocE. This ascribes a contribution of 60–200-fold of rate enhancement to the cocE rate-limiting deacylation step (step B in Mechanism II) (for the limiting role of deacylation in ester hydrolysis by serine hydrolases see⁷). Although the rate-ceiling of the D-Abs may be dictated by an event of a physical nature, a higher 500–2000-fold rate increase was gained by the addition of the exogenous peroxide nucleophile.

In serine hydrolases, deacylation is catalyzed *via* the deprotonation of a resident water molecule to yield a hydroxide anion (Scheme 1, Mechanism II, step B). This deprotonation is catalyzed by the active site His-Asp dyad, which is responsible for deprotonation and activation of the seryl alkoxide reactive nucleophile. A direct measurement of the deacylation rate of acylated chymotrypsin by water gave a rate constant of 77 – 200 s^{-1} . This value, when divided by 55 M, gave a second-order rate constant of 1.4 – $3.6 \text{ M}^{-1} \text{ s}^{-1}$ that is clearly below the second-order rate calculated for peroxide reactivity with the D-Abs, $6 \times 10^5 \text{ M}^{-1} \text{ s}^{-1}$ (determined from the saturated $k_{\text{cat}}^{\text{max}} = 6 \text{ s}^{-1}$ at $10 \mu\text{M}$ peroxide anion concentration; Figure 6).^{7,49} The rate of deacylation of acylated chymotrypsin is enhanced in the presence of α -nucleophiles (hydrazine) but the increase is relatively modest (ca twofold) *versus* that observed with the D-Abs and peroxide (500–2000-fold). Moreover, in the case of chymotrypsin, ordinary amine nucleophiles

(not α -nucleophiles) exhibit higher rates than hydrazine. The highest deacylation rate, observed with tyrosinamide ($1.7 \times 10^4 \text{ M}^{-1} \text{ s}^{-1}$),⁴⁹ is quite close to the rate of the D-Abs with peroxide ($6 \times 10^5 \text{ M}^{-1} \text{ s}^{-1}$). In the former, the high rate reflects the high level of specificity of chymotrypsin for the leaving group (as inferred from the principle of microscopic reversibility),⁴⁹ whilst the latter results from the increased chemical reactivity of the peroxide nucleophile and the high complementarity of the D-Abs to the oxyanionic TS of the reaction.

The maximal rate obtained by the D-Abs ($k_{\text{cat}}^{\text{max}} = 6 \text{ s}^{-1}$) is comparable to that of many esterolytic enzymes (e.g. cocE (Table 5), thioesterases²⁰ and lipases¹⁹). Assuming that deacylation is rate-limiting in these enzymes, a potent exogenous nucleophile at the active site of the D-Abs can match the rate contribution provided to deacylation by the general-base His-Asp dyad in the active site of these enzymes. Nonetheless, in addition to the oxyanionic TS stabilization and the endogenous nucleophilic attacks, other forces may contribute to the fast rates exhibited by esterases. AChE, for example, exhibits a rate acceleration of about 10^{13} . Harel *et al.* suggested that the extraordinary proficiency of AChE is derived from perfectly aligning the substrate for the nucleophilic attack to take place.⁶ Indeed, AChE with its k_{cat} of 10^4 s^{-1} stands out from most other esterases, which exhibit k_{cat} values in the range of 1 – 200 s^{-1} .

Conformational changes

The observation and role of conformational changes in enzymes are often concealed by other rate-determining steps.⁷ In the case of AChE, a rate-limiting induced-fit step was reported with activated aryl substrates, although its role remains unclear.^{8,9} Thioesterase I (Tep-I) represents another example of a natural hydrolase where conformational flexibility was observed but not assigned to function.⁵⁰ For the D-Abs, however, an induced-fit isomerisation was shown to increase the affinity towards the TSA by 60-fold.³⁰ The results presented here indicate that the increase in affinity towards the TSA may be mirrored in the stabilization of the TSs of the esterolytic reaction, hence linking the observed conformational changes to the catalytic mechanism of the D-Abs.

On the generation of more potent esterolytic antibodies

Rivaling the rates of enzyme catalysis, by catalytic antibodies or any other enzyme-mimic, is a daunting challenge.⁵¹ Our results suggest that enzyme-like rates are achievable with esterolytic antibodies, provided that the nucleophilic attack at the antibody active site is made more effective than in bulk solution. One way pointed out by this study is to optimize the electrostatic properties

of the channel through which the nucleophile approaches the active-site, perhaps by engineering positively-charged residues in and around this channel without interfering with the properties of the active-site core.⁵² Recently, antibodies (regardless of their binding specificity) were found to mediate the conversion of singlet oxygen to peroxide.⁵³ It may be possible to elicit antibodies that channel the *in situ* generated peroxide directly into the active site. All these modifications could, in principle, be additive to improvements of the active site itself obtained by increasing the affinity to the TSA.^{3,54} Although catalysis *via* a covalent enzyme-substrate intermediate is not always, or necessarily, an effective route,⁷ an alternative way to faster rates would be *via* Mechanism II involving endogenous active-site nucleophiles, as is the case with most esterolytic enzymes. A few esterolytic antibodies follow this mechanism^{22,23} but, as the hydrolysis of their acyl-antibody intermediate is catalyzed by the rate-limiting attack of an exogenous hydroxide nucleophile, their rates are comparable to esterolytic antibodies that apply Mechanism I.³ Thus, in analogy to natural esterases, introducing a general base to the active site would be highly beneficial. The catalytic rates of antibodies appear to be limited by physical events, such as product release or conformational isomerism.⁵⁵ A significant enhancement in rate may therefore require a parallel improvement of the catalytic machinery and the antibody's dynamics. Most of the improvements suggested above are not likely to be achieved by designing new immunizing haptens or engineering existing antibodies. Thus, the most general and effective way of improving potency would be to select esterolytic antibodies directly for higher rates and turnover.^{30,56} Such direct selections can affect all the factors concerned: those linked directly with the active site (e.g. inducing endogenous active-site nucleophiles) and those peripheral to it (e.g. improving the approach of exogenous nucleophiles or the rate of conformational isomerism).

Materials and Methods

Materials

The generation and purification of the D-antibodies and their recombinant Fv fragments as well as synthesis of transition state analogs and other compounds are described elsewhere.^{14,15,29,30} Fv fragment mutagenesis at positions H100d and L34 was carried out using a Chameleon double-stranded, site-directed mutagenesis kit (Stratagene, La Jolla, CA).

Kinetics

In light of the high **2p** ester background, hydrolysis rates at basic pH and in the presence of high concentrations of α -nucleophiles, initial experiments were carried out to determine the combination of antibody and substrate concentrations that would allow quantitative

measurements. Ester **2p** hydrolysis was monitored by the release of *p*-nitrophenolate (**4p**) at 415 nm as described.¹⁵ All antibody-catalyzed rates are “net”-rates, i.e. the rates observed in the presence of the antibody minus the rate observed under the same conditions with no antibody.

pH dependency

The pH-dependency of ester **2p** (50 μM) hydrolysis by D2.3 \dagger (1 μM) and D2.4 (0.6 μM) was determined in 50 mM sodium borate (pH 7–10) or sodium carbonate (pH 9.5–10.5) buffers with 150 mM NaCl.

The fit of net rates to pH (Figure 2) includes the nucleophile's concentration as generally given in equation (1):

$$[\text{Nu}^-] = \{[\text{Nu}]_{\text{total}} \times 10^{(\text{pH}-\text{p}K_a)}\} / \{1 + 10^{(\text{pH}-\text{p}K_a)}\} \quad (1)$$

However, for hydroxide and peroxide, $\text{p}K_a \gg \text{pH}$, and consequently:

$[\text{Nu}^-] \approx [\text{Nu}]_{\text{total}} \times 10^{(\text{pH}-\text{p}K_a^{\text{Nu}})}$. As $[\text{Nu}]_{\text{total}}$ and $10^{(-\text{p}K_a^{\text{Nu}})}$ are constant, $[\text{Nu}^-] \propto 10^{(\text{pH})}$, and hence, $\log[\text{Nu}^-] \propto \text{pH}$. This accounts for the linear-phase observed in Figure 2 during which: $\log(v_0) \propto [\text{OH}^-]$ or $[\text{O}_2\text{H}^-]$.

The antibody deprotonation step is governed by $\text{p}K_a^{\text{Ab}}$ and is described by⁷:

$$\log(v_0) \propto [\text{AbH}] = [\text{Ab}]_{\text{total}}[\text{H}^+] / (K_a^{\text{Ab}} + [\text{H}^+])$$

The overall rate equation applied to fit the pH-rate profiles in Figure 2 includes both the nucleophile and the antibody concentration terms to give:

$$\log(v_0) = C - \log(10^{(-\text{p}K_a^{\text{Ab}})} + 10^{(-\text{pH})}) \quad (2)$$

where C is a constant that incorporates $[\text{Nu}]_{\text{total}}$, $\text{p}K_a^{\text{Nu}}$ and $[\text{Ab}]_{\text{total}}$.

Nucleophile effect on D-Abs catalysis

Ester **2p** (75 μM) hydrolysis in the presence of 0–10 mM azide, hydroxylamine, hydrazine or peroxide was measured in PBS (pH 7.05) with antibodies D2.3 (1 μM) or D2.4 (0.2 μM). Nucleophile concentrations were corrected to their unprotonated-active form using equation (1). Stopped-flow (Applied Photophysics) measurements of ester **2p** (75 μM) hydrolysis at 405 nm were performed in PBS (pH 7.05) in the presence of peroxide ($[\text{Nu}]_{\text{total}} = 0\text{--}200$ mM) and 1 μM D-Abs \dagger . Initial rates measured in volts/second were converted to $\mu\text{M}/\text{second}$ via a *p*-nitrophenolate calibration curve. Rates were averaged from four to ten independent samples and k_{cat} at different concentrations of peroxide was derived using the Michaelis–Menten model and a K_M

value of 23 μM (K_M for **2p** appears to be unaffected by peroxide; data not shown).

Binding pH profiles

Binding pH profiles were determined by ELISA.¹⁵ Briefly, plates were coated with 2–10 $\mu\text{g}/\text{ml}$ of bovine serum albumin (BSA)-conjugated anilide **5p**, amide **5b**, and phosphonates **1p** or **1b**. The D-Abs were serially diluted in the buffers used in the pH-rate profiling and incubated in the plate for one hour. The plates were rinsed and the amount of bound antibody determined with peroxidase-labeled goat anti mouse Fab antibodies. Antibody titer at each pH value was determined by the antibody dilution leading to 50% binding. This was correlated to the maximal activity at the plateau range (pH < 9) taken as 100%.

Activity of Fv mutants

Competitive ELISA was applied to determine the relative affinities of the D-Abs Fv fragment mutants to TSA **1p** as compared to the binding activity of the wild-type. The Fvs (diluted in 1% (w/v) skim milk powder in TBS (pH 8.3) to a concentration giving 50% binding signal under the same ELISA conditions) were pre-incubated for one hour with or without serially diluted TSA **1p**. Aliquots of these solutions were then applied for one hour at room temperature to ELISA plates coated with 0.5 $\mu\text{g}/\text{ml}$ of **1p**-BSA conjugate¹⁵ followed by detection with anti-E-tag antibody (Pharmacia).²⁹ The concentration of **1p** TSA resulting in 50% inhibition (IC_{50}) was determined for each Fv mutant and correlated to the IC_{50} of the wild-type. The k_{cat} and K_M values of the AsnL34 \rightarrow Gly,Tyr mutants were determined by Michaelis–Menten kinetics as described for the wild-type Fv fragment.²⁹ The poor activity of the AsnL34 \rightarrow Gln and TyrH100d \rightarrow Ser,Lys,Phe,Gly mutants were assayed by titration using catELISA¹⁴ where their signals were compared to the wild-type activity.

Acknowledgments

We deeply thank Dr Miriam Eisenstein for the structural surface-charge calculations. A.B.L. was supported by EMBO and FEBS short-term fellowships. The financial support of the Henry S. and Anne S. Reich research fund is gratefully acknowledged.

References

- Carter, P. & Wells, J. A. (1990). Functional interaction among catalytic residues in subtilisin BPN'. *Proteins: Struct. Funct. Genet.* **7**, 335–342.
- Lerner, R. A., Benkovic, S. J. & Schultz, P. G. (1991). At the crossroads of chemistry and immunology: catalytic antibodies. *Science*, **252**, 659–667.
- Hilvert, D. (2000). Critical analysis of antibody catalysis. *Annu. Rev. Biochem.* **69**, 751–793.
- Stevenson, J. D. & Thomas, N. R. (2000). Catalytic antibodies and other biomimetic catalysts. *Nat. Prod. Rep.* **17**, 535–577.
- Tantillo, D. & Houk, K. (2001). Canonical binding arrays as molecular recognition elements in the

\dagger Slow, minute-scale, substrate-induced conformational changes generate the higher-active form of the antibody in a hysteretic manner manifested by a lag in the kinetics of product release.³⁰ The lag persists in the pH range studied and in the presence of peroxide, suggesting that the equilibrium between the two antibody isomers is unaffected during the time-scale of these kinetics measurements (less than two minutes). Thus, our data reflect the activity of a mixture between the higher and nether-active conformers, dominated by the active isomer.

- immune system: tetrahedral anions and the ester hydrolysis transition state. *Chem. Biol.* **8**, 535–545.
6. Harel, M., Quinn, D. M., Nair, H. K., Silman, I. & Sussman, J. L. (1996). The X-ray structure of a transition state analog complex reveals the molecular origins of the catalytic power and substrate specificity of acetylcholinesterase. *J. Am. Chem. Soc.* **118**, 2340–2346.
 7. Fersht, A. R. (1985). *Enzyme Structure and Mechanism*, Freeman, New York.
 8. Rosenberry, T. L. (1975). Catalysis by acetylcholinesterase: evidence that the rate-limiting step for acylation with certain substrates precedes general acid–base catalysis. *Proc. Natl Acad. Sci. USA*, **72**, 3834–3848.
 9. Acheson, S. A., Depopoulou, D. & Quinn, D. M. (1987). Simple general acid–base catalysis and virtual transition states for acetylcholinesterase-catalysed hydrolysis of ester substrates. *J. Am. Chem. Soc.* **109**, 239–245.
 10. Wang, L., Pang, Y., Holder, T., Brender, J. R., Kurochkin, A. V. & Zuiderweg, E. R. (2001). Functional dynamics in the active site of the ribonuclease binase. *Proc. Natl Acad. Sci. USA*, **98**, 7684–7689.
 11. Berger, E., Arabshahi, A., Wei, Y., Schilling, J. F. & Frey, P. A. (2001). Acid–base catalysis by UDP-galactose 4-epimerase: correlations of kinetically measured acid dissociation constants with thermodynamic values for tyrosine 149. *Biochemistry*, **40**, 6699–6705.
 12. Vande Berg, B. J., Beard, W. A. & Wilson, S. H. (2001). DNA structure and aspartate 276 influence nucleotide binding to human DNA polymerase beta. Implication for the identity of the rate-limiting conformational change. *J. Biol. Chem.* **276**, 3408–3416.
 13. Baltzinger, M. & Holler, E. (1982). Kinetics of acyl transfer ribonucleic acid complexes of *Escherichia coli* phenylalanyl-tRNA synthetase. A conformational change is rate limiting in catalysis. *Biochemistry*, **21**, 2460–2467.
 14. Tawfik, D. S., Green, B. S., Chap, R., Sela, M. & Eshhar, Z. (1993). catELISA: a facile general route to catalytic antibodies. *Proc. Natl Acad. Sci. USA*, **90**, 373–377.
 15. Tawfik, D. S., Lindner, A. B., Chap, R., Eshhar, Z. & Green, B. S. (1997). Efficient and selective *p*-nitrophenyl-ester-hydrolyzing antibodies elicited by a *p*-nitrobenzyl phosphonate hapten. *Eur. J. Biochem.* **244**, 619–626.
 16. Charbonnier, J. B., Golinelli, P. B., Gigant, B., Tawfik, D. S., Chap, R., Schindler, D. G. *et al.* (1997). Structural convergence in the active sites of a family of catalytic antibodies. *Science*, **275**, 1140–1142.
 17. Gigant, B., Charbonnier, J. B., Eshhar, Z., Green, B. S. & Knossow, M. (1997). X-ray structures of a hydrolytic antibody and of complexes elucidate catalytic pathway from substrate binding and transition state stabilization through water attack and product release. *Proc. Natl Acad. Sci. USA*, **94**, 7857–7861.
 18. Jencks, W. P. & Carriuolo, J. (1960). Reactivity of nucleophilic agents toward esters. *J. Am. Chem. Soc.* **82**, 1778–1786.
 19. Stoops, J. K., Horgan, D. J., Runnegar, M. T., De Jersey, J., Webb, E. C. & Zerner, B. (1969). Carboxylesterases (EC 3.1.1). Kinetic studies on carboxylesterases. *Biochemistry*, **8**, 2026–2033.
 20. Lee, Y. L., Chen, J. C. & Shaw, J. F. (1997). The thioesterase I of *Escherichia coli* has arylesterase activity and shows stereospecificity for protease substrates. *Biochem. Biophys. Res. Commun.* **231**, 452–456.
 21. Larsen, N. A., Turner, J. M., Stevens, J., Rosser, S. J., Basran, A., Lerner, R. A. *et al.* (2002). Crystal structure of a bacterial cocaine esterase. *Nature Struct. Biol.* **9**, 17–21.
 22. Wirsching, P., Ashley, J. A., Benkovic, S. J., Janda, K. D. & Lerner, R. A. (1991). An unexpectedly efficient catalytic antibody operating by ping-pong and induced fit mechanisms. *Science*, **252**, 680–685.
 23. Krebs, J. F., Siuzdak, G., Dyson, H. J., Stewart, J. D. & Benkovic, S. J. (1995). Detection of a catalytic antibody species acylated at the active site by electrospray mass spectrometry. *Biochemistry*, **34**, 720–723.
 24. Martin, M. T., Napper, A. D., Schultz, P. G. & Rees, A. R. (1991). Mechanistic studies of a tyrosine-dependent catalytic antibody. *Biochemistry*, **30**, 9757–9761.
 25. Angeles, T. S., Smith, R. G., Darsley, M. J., Sugawara, R., Sanchez, R. I., Kenten, J. *et al.* (1993). Isozymes: structurally and mechanistically similar catalytic antibodies from the same immunization. *Biochemistry*, **32**, 12128–12135.
 26. Gigant, B., Tsumuraya, T., Fujii, I. & Knossow, M. (1999). Diverse structural solutions to catalysis in a family of antibodies. *Struct. Fold. Des.* **7**, 1385–1393.
 27. Resmini, M., Vigna, R., Simms, C., Barber, N. J., Hagi-Pavli, E. P., Watts, A. B. *et al.* (1997). Characterization of the hydrolytic activity of a polyclonal catalytic antibody preparation by pH-dependence and chemical modification studies: evidence for the involvement of Tyr and Arg side chains as hydrogen-bond donors. *Biochem. J.* **326**, 279–287.
 28. Tantillo, D. J. & Houk, K. N. (1999). Fidelity in hapten design: how analogous are phosphonate haptens to the transition states for alkaline hydrolyses of aryl esters? *J. Org. Chem.* **64**, 3066–3076.
 29. Kim, S. H., Schindler, D. G., Lindner, A. B., Tawfik, D. S. & Eshhar, Z. (1997). Expression and characterization of recombinant single-chain Fv and Fv fragments derived from a set of catalytic antibodies. *Mol. Immunol.* **34**, 891–906.
 30. Lindner, A. B., Eshhar, Z. & Tawfik, D. S. (1999). Conformational changes affect binding and catalysis by ester-hydrolysing antibodies. *J. Mol. Biol.* **285**, 421–430.
 31. Sela, M. & Mozes, E. (1966). Dependence of the chemical nature of antibodies on the net electrical charge of antigens. *Proc. Natl Acad. Sci. USA*, **55**, 445–452.
 32. Martin, A. C. (1996). Accessing the Kabat antibody sequence database by computer. *Proteins: Struct. Funct. Genet.* **25**, 130–133.
 33. Jencks, W. P. (1958). The reaction of hydroxylamine with activated acyl groups. I. Mechanism of the reaction. *J. Am. Chem. Soc.* **80**, 4585–4588.
 34. Admiraal, S. J., Meyer, P., Schneider, B., Deville-Bonne, D., Janin, J. & Herschlag, D. (2001). Chemical rescue of phosphoryl transfer in a cavity mutant: a cautionary tale for site-directed mutagenesis. *Biochemistry*, **40**, 403–413.
 35. Zhou, G. W., Guo, J., Huang, W., Fletterick, R. J. & Scanlan, T. S. (1994). Crystal structure of a catalytic antibody with a serine protease active site. *Science*, **265**, 1059–1064.
 36. Kimball, A. S., Lee, J., Jayaram, M. & Tullius, T. D. (1993). Sequence-specific cleavage of DNA *via* nucleophilic attack of hydrogen peroxide, assisted by Flp recombinase. *Biochemistry*, **32**, 4698–4701.

37. Viladot, J. L., de Ramon, E., Durany, O. & Planas, A. (1998). Probing the mechanism of *Bacillus* 1,3-1,4-beta-D-glucan 4-glucanohydrolases by chemical rescue of inactive mutants at catalytically essential residues. *Biochemistry*, **37**, 11332–11342.
38. Admiraal, S. J., Schneider, B., Meyer, P., Janin, J., Veron, M., Deville-Bonne, D. & Herschlag, D. (1999). Nucleophilic activation by positioning in phosphoryl transfer catalyzed by nucleoside diphosphate kinase. *Biochemistry*, **38**, 4701–4711.
39. Hori, T., Kumasaka, T., Yamamoto, M., Nonaka, N., Tanaka, N., Hashimoto, Y. *et al.* (2001). Structure of a new aspzincin metalloendopeptidase from *Grifola frondosa*: implications for the catalytic mechanism and substrate specificity based on several different crystal forms. *Acta Crystallog. sect. D*, **57**, 361–368.
40. Szeltner, Z., Renner, V. & Polgar, L. (2000). Substrate- and pH-dependent contribution of oxyanion binding site to the catalysis of prolyl oligopeptidase, a paradigm of the serine oligopeptidase family. *Protein Sci.* **9**, 353–360.
41. Vazeux, G., Iturrioz, X., Corvol, P. & Llorens-Cortes, C. (1997). A tyrosine residue essential for catalytic activity in aminopeptidase A. *Biochem. J.* **327**, 883–889.
42. Bryan, P., Pantoliano, M. W., Quill, S. G., Hsiao, H. Y. & Poulos, T. (1986). Site-directed mutagenesis and the role of the oxyanion hole in subtilisin. *Proc. Natl Acad. Sci. USA*, **83**, 3743–3745.
43. O'Connell, T. P., Day, R. M., Torchilin, E. V., Bachovchin, W. W. & Malthouse, J. G. (1997). A 13C-NMR study of the role of Asn-155 in stabilizing the oxyanion of a subtilisin tetrahedral adduct. *Biochem. J.* **326**, 861–866.
44. Menard, R., Carriere, J., Laflamme, P., Plouffe, C., Khouri, H. E., Vernet, T. *et al.* (1991). Contribution of the glutamine 19 side chain to transition-state stabilization in the oxyanion hole of papain. *Biochemistry*, **30**, 8924–8928.
45. Nicolas, A., Egmond, M., Verrips, C. T., de Vlieg, J., Longhi, S., Cambillau, C. & Martinez, C. (1996). Contribution of cutinase serine 42 side chain to the stabilization of the oxyanion transition state. *Biochemistry*, **35**, 398–410.
46. Juhasz, T., Szeltner, Z., Renner, V. & Polgar, L. (2002). Role of the oxyanion binding site and subsites s1 and s2 in the catalysis of oligopeptidase B, a novel target for antimicrobial chemotherapy. *Biochemistry*, **41**, 4096–4106.
47. Carlos, J. L., Klenotic, P. A., Paetzel, M., Strynadka, N. C. & Dalbey, R. E. (2000). Mutational evidence of transition state stabilization by serine 88 in *Escherichia coli* type I signal peptidase. *Biochemistry*, **39**, 7276–7283.
48. Bresler, M. M., Rosser, S. J., Basran, A. & Bruce, N. C. (2000). Gene cloning and nucleotide sequencing and properties of a cocaine esterase from *Rhodococcus* sp. strain MB1. *Appl. Environ. Microbiol.* **66**, 904–908.
49. Fastrez, J. & Fersht, A. R. (1973). Demonstration of acyl-enzyme mechanism for the hydrolysis of peptides and anilides by chymotrypsin. *Biochemistry*, **12**, 2025–2034.
50. Huang, Y. T., Liaw, Y. C., Gorbatyuk, V. Y. & Huang, T. H. (2001). Backbone dynamics of *Escherichia coli* thioesterase/protease I: evidence of a flexible active-site environment for a serine protease. *J. Mol. Biol.* **307**, 1075–1090.
51. Kirby, A. J. (1996). Enzyme mechanisms, models, and mimics. *Angew. Chem., Int. Ed. Engl.* **35**, 707–724.
52. Selzer, T., Albeck, S. & Schreiber, G. (2000). Rational design of faster associating and tighter binding protein complexes. *Nature Struct. Biol.* **7**, 537–541.
53. Wentworth, A. D., Jones, L. H., Wentworth, P., Jr, Janda, K. D. & Lerner, R. A. (2000). Antibodies have the intrinsic capacity to destroy antigens. *Proc. Natl Acad. Sci. USA*, **97**, 10930–10935.
54. Takahashi, N., Kakinuma, H., Liu, L., Nishi, Y. & Fujii, I. (2001). *In vitro* abzyme evolution to optimize antibody recognition for catalysis. *Nature Biotechnol.* **19**, 563–567.
55. Stewart, J. D. & Benkovic, S. J. (1995). Transition-state stabilization as a measure of the efficiency of antibody catalysis. *Nature*, **375**, 388–391.
56. Griffiths, A. D. & Tawfik, D. S. (2000). Man-made enzymes—from design to *in vitro* compartmentalisation. *Curr. Opin. Biotechnol.* **11**, 338–353.
57. Yang, A. S., Gunner, M. R., Sampogna, R., Sharp, K. & Honig, B. (1993). On the calculation of pK_as in proteins. *Proteins: Struct. Funct. Genet.* **15**, 252–265.
58. Landry, D. W., Zhao, K., Yang, G. X., Glickman, M. & Georgiadis, T. M. (1993). Antibody-catalyzed degradation of cocaine. *Science*, **259**, 1899–1901.

Edited by I. Wilson

(Received 21 November 2001; received in revised form 24 April 2002; accepted 25 April 2002)